Published in final edited form as:
Cancer Gene Ther. 2012 June ; 19(6): 393–401. doi:10.1038/cgt.2012.12.

Targeted therapy via oral administration of attenuated *Salmonella* expression plasmid-vectored Stat3-shRNA cures orthotopically transplanted mouse HCC

Y Tian[1,7], **B Guo**[2,7], **H Jia**[1], **K Ji**[1], **Y Sun**[3], **Y Li**[1], **T Zhao**[1], **L Gao**[1], **Y Meng**[1], **DV Kalvakolanu**[4], **DJ Kopecko**[5], **X Zhao**[3], **L Zhang**[1], and **D Xu**[6]

L Zhang: zhangling3@jlu.edu.cn; D Xu: dqxujl@gmail.com

[1]Prostate Diseases Prevention and Treatment Research Centre and Department of Pathophysiology, Norman Bethune College of Medicine, Jilin University, Changchun, People's Republic of China

[2]Department of Emergency Medicine, China-Japan Union Hospital of Jilin University, Changchun, People's Republic of China

[3]The First Hospital of Jilin University, Changchun, People's Republic of China

[4]Greenebaum Cancer Center, Department of Microbiology and Immunology, Molecular Biology Program, University of Maryland School Medicine, Baltimore, MD, USA

[5]Laboratory of Enteric and Sexually Transmitted Diseases, Center for Biologics Evaluation and Research, Food and Drug Administration, Bethesda, MD, USA

[6]New Vaccine National Engineering Research Center, Beijing, People's Republic of China

Abstract

The development of RNA interference-based cancer gene therapies has been delayed due to the lack of effective tumor-targeting delivery systems. Attenuated *Salmonella enterica* serovar Typhimurium (*S.* Typhimurium) has a natural tropism for solid tumors. We report here the use of attenuated *S.* Typhimurium as a vector to deliver shRNA directly into tumor cells. Constitutively activated signal transducer and activator of transcription 3 (*Stat3*) is a key transcription factor involved in both hepatocellular carcinoma (HCC) growth and metastasis. In this study, attenuated *S.* Typhimurium was capable of delivering shRNA-expressing vectors to the targeted cancer cells and inducing RNA interference *in vivo*. More importantly, a single oral dose of attenuated *S.* Typhimurium carrying shRNA-expressing vectors targeting Stat3 induced remarkably delayed and reduced HCC (in 70% of mice). Cancer in these cured mice did not recur over 2 years following treatment. These data demonstrated that RNA interference combined with *Salmonella* as a delivery system may offer a novel clinical approach for cancer gene therapy.

Keywords

HCC; immune response; RNA interference; Stat3

Correspondence: Professor L Zhang, Prostate Diseases Prevention and Treatment Research Centre and Department of Pathophysiology, Norman Bethune College of Medicine, Jilin University, Changchun 130021, Jilin, People's Republic of China or Professor D Xu, New Vaccine National Engineering Research Center, Beijing, People's Republic of China.
[7]These authors contributed equally to this work.

CONFLICT OF INTEREST

The authors declare no conflict of interest.

INTRODUCTION

Hepatocellular carcinoma (HCC) is the sixth most common cancer in the world,[1] and the prognosis is poor because of rapid tumor progression and recurrence.[2] It is characterized as an inherently chemotherapy-resistant cancer and there are no well-established effective systemic therapies until now.[3] Currently, several signaling pathways critical for HCC pathogenesis have been recognized, such as the Ras/Raf/MEK/ERK pathway and PI3K/Akt/mTOR pathway,[4,5] and the transcription factor signal transducer and activator of transcription 3 (*Stat3*) signaling pathway is reported to have a key role in HCC growth and metastasis.[6] Thus, targeting this pathway may lead to an effective treatment to HCC.

RNA interference is a powerful research tool for cancer gene silencing.[7] However, a key obstacle to the development of RNA interference-based cancer gene therapies is targeted delivery to cancer cells.[8] *Salmonella enterica* serovar Typhimurium (*S*. Typhimurium) has a natural tropism, not only for solid tumors but also for metastatic lesions in mice, and accumulates at greater than 10 000 times more in the tumor tissues than normal tissues.[9] We have previously employed a delivery system involving attenuated *S.* Typhimurium combined with silencing shRNA expression plasmids as a therapeutic treatment for prostate cancer.[10] As the liver and spleen are natural targets of *S.* Typhimurium in mice after oral ingestion,[11] we hypothesized that attenuated *S.* Typhimurium carrying Stat3-shRNA-expressing vectors will be effective in treating HCC. Our results indicate that a single dose of attenuated *S.* Typhimurium expressing Stat3-shRNA effects a synergistic suppression of both HCC growth, metastases and elicits multi-component antitumor immunity. Most significantly, HCC was eradicated from 70% of mice and did not recur within 2 years following treatment.

MATERIALS AND METHODS

Plasmids, bacteria, cell culture and animals

Double-stranded DNA oligonucleotides were cloned into pGCsilencerU6/Neo/GFP, which also expresses a green fluorescent protein (*GFP*) gene (GeneChem, Shanghai, China), to generate plasmids pSi-Stat3 and pSi-Scramble as described previously.[10] The attenuated *S.* Typhimurium phoP/phoQ null strain LH430 was kindly provided by Dr EL Hohmann.[12] Plasmids were electroporated into *Salmonella* before use. Mouse H22 hepatoma cells, obtained from the Shanghai Institute of Cell Biology, Chinese Academy of Sciences (Shanghai, China), were cultured in RPMI 1640 containing 10% fetal bovine serum in a humidified atmosphere at 37 °C in 5% CO_2. All culture media were purchased from the Life Technologies, (Gaithersburg, MD). C57BL6 mice, weighing 18 – 22 g, were purchased from the Beijing Institute for Experimental Animals. All animals were housed and experiments were performed in accordance with the guidelines set out by the Animal Experimental Ethics Committee of Jilin University.

Establishment of orthotopically implanted hepatocarcinoma tumor model

In all, 0.2 ml (1×10^8 per ml) H22 cell solution was subcutaneously inoculated to form ectopic transplanted model in mice to form a solid tumor. After 10 days, when tumors of 3 – 5 mm in diameter formed in the right groin of these mice, they were removed and sheared into small pieces of 1 mm^3 under sterile conditions. C57BL6 mice were anesthetized by coelio-injection of Pentobarbitone (70 mg kg^{-1}) and laparotomy was performed. Under sterile conditions the right lobes of liver were punctured to form a 3-mm-long sinus tract and a small piece of tumor tissue was put into each sinus tract, and the orthotopic transplantation tumor model of HCC was established.

Antitumor activity of recombinant *Salmonella* on established tumor model of HCC

Seven days after orthotopic tumor implantation, mice were randomly divided into three groups (n = 10 per group). Before treatment, all mice were starved overnight and orally pre-administered with 100 μl of 10 g l^{-1} $NaHCO_3$ solution half an hour before inoculation. Each time, 100 μl PBS (pH 7.6) was given to the mice in the mock group, and 1×10^8 cfu of recombinant *S.* Typhimurium carrying different plasmids were given to mice by orogastric inoculation. The orthotopic transplantation tumors were observed by Philips HDI-4000 color Doppler ultrasound (CA, USA). Mice were killed 21 days after administration of bacteria; tumors were excised, weighed and measured for tumor diameter of tumors. The HCC tissues, adjacent non-cancerous liver tissues, lung tissues and lymph nodes were sampled and fixed in 10% formalin to determine metastases. For long-term observation of survival rate, another 30 mice were treated in a similar fashion and followed over 2 years.

Analysis of bacterial distribution and clearance

Tumor, liver, spleen, heart and lung tissues from control or bacterially treated mice were excised, weighed and homogenized. The diluted tissue homogenates were observed by flow cytometry. Green fluorescence was observed in bacterially infected cells. A portion of each tissue was also prepared for transmission electron microscopic analysis to determine the extent of bacterial infection.

Semi-quantitative RT-PCR

Total RNA was isolated from the transfected cells and control cells using Trizol reagent (Gibco BRL, Gaithersburg, MD, USA) as described by the manufacturer. The cDNA was synthesized using a Takara RNA PCR Kit (TaKaRa, Tokyo, Japan). Primers used in PCR were as in Table 1.

The PCR products were analyzed by standard agarose gel electrophophoresis, and the bands were quantified using BandLeader 3.0 software (Magnitec Ltd, Tel Aviv, Israel). Semiquantitative analysis of RT-PCR products was accomplished by computerized optical densitometry of the bands.

Western blotting and immunohistochemical analyses

Cell lysis, protein quantification, western blot and immunohistochemical analyses were carried out as described previously.[13,14] Antibodies against STAT3, phospho-Tyr^{705}-Stat3 (p-Stat3), cyclin D1, c-Myc, vascular endothelial growth factor, HIF-1, β-actin and antimouse MMP-2 (Santa Cruz Biotech, Heidelberg, Germany), Bcl-2 (DAKO Biotech, Carpinteria, CA, USA), and Ki-67 (Biogenex, Fremont, CA, USA) were used. Protein bands were detected with enhanced chemiluminescence western blotting reagents (Amersham, Buckinghamshire, UK).

Analysis of apoptosis and cell cycle

After treatment, the portion of tumor tissue was homogenized and apoptosis was analyzed subsequently using the Annexin V-FITC kit (Keygen Biotech, Nanjing, China) according to the protocol described by the manufacturer. The results were analyzed by fluorescence microscopy (FACScan, Becton Dickinson, Franklin Lakes, NJ) at 24 h and 15 days. Fresh tumor tissues were fixed, dehydrated, embedded, cut into ultrathin sections and stained. Samples were examined under a Philips CM 12 transmission electron microscope (TEM) to detect apoptosis as described previously.[15] Cell cycle phase distribution was determined by flow cytometry and tumor tissue sections from animals were used for H&E staining and terminal deoxynucleotidyl transferase-mediated nick-end labeling (TUNEL) assays, as described previously.[13]

Flow cytometry analysis

At selected time points after tumor inoculation, tumor-bearing animals were killed and spleens were isolated. Spleens were homogenized by mechanical dispersion to a cell suspension in flow cytometry buffer. The supernatant of the splenocytes after filtering through cell filter membrane were stained with appropriate fluorescence-conjugated antibodies to CD3, CD4, CD8, CD80, CD86, MHC II, NK1.1 or their respective isotype controls and incubated for 30 min at 4 °C. CD25 and Foxp3 T cells were detected using the mouse Treg cell staining kit (eBioscience, San Diego, CA, USA).

Lymphocyte proliferation

Mouse splenic lymphocytes (5×10^5cells per 100 μl per well) were incubated in the absence or presence of ConA (5 mg ml^{-1}) in a 96-well plate in triplicate for 72 h. In all, 20 μl MTT (5 mg ml^{-1}, Invitrogen, Carlsbad, CA) was added and cells were cultured for additional 4 h. Subsequently, cells were lysed using dimethylsulfoxide (150 μl per well, Pierce Biotechnology, Rockford, IL, USA). When the formanzan crystals were completely dissolved, the optical density (OD) was measured at 490 nm using a enzyme micro-plate reader (Microplate Reader Model 550, Bio-Rad, Shanghai, China). The stimulation index (SI) was calculated according to the following formula: $\mathrm{SI}=\mathrm{OD}_{\text{Con A}-\text{stimulated lymphocyte proliferation}}/\mathrm{OD}_{\text{spontaneous lymphocyte proliferation without Con A}}$. SI>2 was regarded as a positive result provided that lymphoblasts were present in the stimulated culture.

NK cytotoxicity assay

NK cells from mouse spleens were prepared as described above and used as effector cells. YAC-1 cells, mouse lymphoma sensitive to NK cells were used as target cells. The YAC-1 cells were washed twice, counted and adjusted to 1×10^5 per ml. Briefly, 100 μl of YAC-1 (1×10^4 cells) were added to each well of a 96-well plate, and 100 μl of each concentration of the effector cells were added to form mixtures with various E:T ratios (50:1, 25:1 and 12.5:1). After a 16-h incubation at 370 °C, NK cytotoxicity tests were used for MTT assay as described above. The cytotoxic activity in each E:T ratio was calculated as follows: $\text{NK cytotoxicity}\% = [1-(\mathrm{OD}_{\text{effector+target cells}})-(\mathrm{OD}_{\text{effector cells}})]/(\mathrm{OD}_{\text{target cells}})\times\%$. Data are presented as the mean of triplicate samples±s.e.m.

Statistical analysis

Data were presented as the mean±s.d. per group. Statistical analysis was made for multiple comparisons using analysis of variance and Student's *t*-test. All experiments were repeated three times. *P*-value <0.05 (SPSS10.0 statistical software, Lebanon, IN, USA) was considered statistically significant.

RESULTS

Localization of *Salmonella* in tumor and other tissues

Following oral administration, the accumulation of attenuated *S.* Typhimurium was evaluated in various tissues at specified times by flow cytometry. Some levels of GFP expression could be detected in all tissues. Figure 1a shows that at 24 h after inoculation attenuated *Salmonella* accumulated predominantly in the liver, spleen and the H22 tumor, but was also detected in the heart, lung and kidneys. The number of bacteria increased in the tumor and the liver and decreased in the spleen at 5 and 10 days after administration. By day 30, the number of attenuated *S.* Typhimurium in the tumor remained significantly higher than other tissues. Figure 1b shows that the *GFP*-expressed bacterial distributions in tumor tissues were noticeably stronger than in normal liver tissues at day 30, around 13.7-fold.

TEM analyses within tumor cells revealed attenuated *S.* Typhimurium in the intercellular spaces in tumors and in tumor-associated macrophages. These results indicate that attenuated *S.* Typhimurium can specifically home to tumor cells, possibly via tumor-associated macrophages. Inhibition of orthotopically transplanted liver tumor growth and metastasis *in vivo* by therapeutic treatment of bacterially delivered shRNAs

In order to evaluate the antitumor ability of recombinant *S.* Typhimurium, we employed a C57BL6 mouse orthotopic liver tumor implant model. Fifteen days after tumor implantation, mice were divided into four groups (n =10 per group) and then injected with 1×10^7 cfu of attenuated *S.* Typhimurium carrying different plasmids via orogastric inoculation. Twenty days after bacterial inoculation, mice were sacrificed, and the tumors were excised, weighed and measured. As shown in Table 2, mice treated with buffer alone (mock control) developed primary tumors with a mean volume of 2274.09±1735.17 mm^3. In mice treated with *Salmonella*-Si-scramble, tumors grew to a volume of 551.98±367.01 mm^3, similar to the tumor volume of mice treated with *S.* Typhimurium without any plasmid. However, mice treated with *Salmonella*-Si-Stat3 developed tumors with a median reduced volume of 301.99±390.16 mm^3 and showed marked tumor growth suppression compared with the *Salmonella*-Si-scramble or *Salmonella* alone (P<0.05). Remarkably, tumors completely disappeared in 70% of mice in this group over 20 days (Figures 2a–c). Observation of metastases of implanted tumors revealed that in the animals treated with *Salmonella*-Si-Stat3, intraceliac seeding, bloody ascites and lung metastases were all significantly decreased compared with buffer alone-treated mice (Table 2). These data directly demonstrate that the attenuated *Salmonella* expressing a Stat3-specific siRNA exerts a strong antitumor and anti-metastasis effect.

Survival time extension of mice bearing orthotopic liver tumors by therapeutic treatment with bacterially delivered shRNAs

To further demonstrate the therapeutic utility of *Salmonella*-delivered shRNAs, tumor-bearing mice were orally administered *S.* Typhimurium carrying various plasmids or buffer. Mice were observed for 2 years. As shown in Figure 2d, all mice (n =10) injected with buffer were dead before 40 days. In contrast, the mice treated with *Salmonella*-Si-Stat3 and *Salmonella*-Si-Scramble significantly extended mean survival times and had seven and four surviving mice at 2 years without tumor recurrence, respectively. Thus, therapeutic treatment with bacterially delivered shRNAs significantly prolong the survival time of H22 tumor mice.

Specific reduction of Stat3 expression by *Salmonella*-delivered siRNAs in orthotopic liver tumor implants

A reduction of *Stat3* mRNA and protein was observed by using semi-quantitative RT-PCR and western blotting analyses 15 days after bacterial inoculation. Administration of *Salmonella*-Si-Stat3 reduced the *Stat3* mRNA level to 30% of the *Salmonella*-Si-Scramble (Figures 3a and b). Western blotting analyses with native Stat3 (Stat3)- and phosphorylated Tyr705 Stat3 (p-Stat3)-specific antibodies also showed a strong inhibition of p-Stat3 or Stat3 proteins to 18% or 5%, respectively, following treatment with *Salmonella*-Si-Stat3 (Figure 3c and d) compared with *Salmonella*-Si-Scramble. Immunohistochemical analyses for Stat3 expression in the H22 tumors treated with buffer or *Salmonella*-Si-Scramble were highly positive for Stat3. In contrast, H22 tumor cells treated with *Salmonella*-Si-Stat3 stained weakly for Stat3 (Figure 4b). Therefore, the expression of Stat3 and p-Stat3 is specifically knocked down by *Salmonella*-delivered Si-Stat3.

Induction of apoptosis and G1 arrest by *Salmonella*-delivered siRNAs

To study the therapeutic mechanism of bacterially delivered shRNAs, H22 tumor tissues were subjected to flow cytometry and TUNEL staining. Flow cytometric analysis by Annexin V-FITC showed that *Salmonella*-Si-Stat3 induced significant apoptosis compared with the Si-Scramble controls at 24 h (~9.4-fold) and at 15 days (~10.2-fold) (Figure 4a). A further analysis of the flow cytometry data showed that the *Salmonella*-Si-Stat3-treated cells accumulated significantly in G1 phase compared with the control (69.1±2.89% versus 47.5±2.25%, $P<0.05$) (data not shown). The percentage of TUNEL-positive liver cancer cells in *Salmonella*-Si-Stat3 group was significantly higher than that in *Salmonella*-Si-Scramble group (apoptosis index was 32.3±4.1 versus 7.8±5.3%, $P<0.01$, Figure 4c). TEM revealed abundant chromatin condensation, fragmentation and apoptotic body in *Salmonella*-Si-Stat3-treated cells (Figure 4c). These data suggest that *Salmonella*-delivered Si-Stat3 treatment can inhibit H22 tumor growth by inducing apoptosis and locking tumor cells in the G1 phase.

Reduction of Stat3-downstream targeted genes by *Salmonella*-delivered shRNAs

As Stat3 significantly regulates H22 tumor growth and metastases, we next examined the expression of Stat3-downstream targeted genes by using semi-quantitative RT-PCR, western blotting and immunohistochemical analyses. Following *Salmonella*-Si-Stat3 treatment, antiapoptotic *Bcl-2*, inducers of tumor angiogenesis *VEGF* and a master regulator for surviving hypoxia of carcinoma *HIF-1* mRNAs and proteins were reduced and cell cycle regulators cyclin D1, and c-Myc were also diminished (Figure 5). Ki-67 (a cell division – associated antigen) and MMP-2, known to promote metastasis, were also suppressed by treatment with *Salmonella*-Si-Stat3 compared with the Si-Scramble control (Figure 4d). Caspase-3, a key mediator of apoptosis, stained significantly stronger in the *Salmonella*-Si-Stat3 group than scrambled vector (Figure 4b). These results show that *Salmonella*-Si-Stat3 inhibits the expression of Stat3 and Stat3-regulated genes, and results in a stronger suppression of tumor proliferation via apoptosis and metastases inhibition.

Salmonella-delivered Stat3 siRNAs enhanced NK cells activity of tumor-beared mouse

To determine the impact for NK cells *in vivo* by *Salmonella*-Si-Stat3, we measured the antitumor activity by NK cytotoxicity assay. As a result, the NK cell activity of *Salmonella*-Si-Stat3 group at the E:T ratio 25:1, 50:1 and 100:1 was 47.7%, 70.5% and 71.9%, respectively (Figure 6a). The NK cell activity for *Salmonella*-Si-Stat3 group was significantly higher than that of mock group ($P<0.05$). As shown by flow cytometry for the expression of activation markers, treatment with the *Salmonella*-Si-Stat3 group significantly upregulates the number of NK cells in comparison with the mock group (Figure 6b).

Salmonella-delivered Stat3 siRNAs modulated T lymphocytes function of tumor-beared mouse

On days 21 of treatment, MTT assay was performed to evaluate the lymphocyte proliferation induced by Con A. The results indicate that both *Salmonella*-Si-scramble or *Salmonella*-Si-Stat3 group had no obvious influence on splenic lymphocyte proliferation at the concentration of 5 $\mu g\ ml^{-1}$ Con A, but lymphocyte proliferation was elevated when stimulated with the concentration of 10 $\mu g\ ml^{-1}$ Con A. However, the stimulation index (SI) was significantly increased in *Salmonella*-Si-Stat3 group with the concentration of 20 $\mu g\ ml^{-1}$ Con A compared to the control group (Figure 6c) ($P<0.01$). Moreover, the $CD3^{+}$/ $CD8^{+}$ T cells were further analyzed for three-color flow cytometry. The results showed that the percentage of $CD8^{+}$ T cells were successively increased by *Salmonella*-Si-Stat3-treated mice (Figure 6d). As eradication of tumors, is thought to be inhibited by T-regulatory (Treg) cells, we examined whether Stat3 deficiency might affect Treg cells. Indeed, the proportions

of CD4 $^{+}$ T cells expressing Treg markers (CD25 and Foxp3) in the *Salmonella*-Si-Stat3 group were considerably reduced (Figures 6e and f), which account for approximately 30 and 60% of the mock group separately. Changes in Treg cells might be the result of Stat3 deficiency in T cells or indirect effects influenced by Stat3 signaling in other immune cells.

DISCUSSION

RNA interference therapy has recently been used successfully to knock down abnormally upregulated specific cancer gene expression.[16,17] In addition, challenge to the practical application of RNA interference therapy in human tumors is to define a targeted method of siRNA delivery specifically to reach the cytoplasm of cancer cells.[8,18] Systemic delivery systems such as retrovirus or adenovirus can target tumor cells well, but are limited to research use in animal models due to human safety issues.[19,20] Certain bacteria have great potential as siRNA delivery vectors and have already been employed in animals and humans.[21 – 23] *S.* Typhimurium is an intracellular bacterial pathogen that mainly invades mucosa-associated lymphoid tissue through M cells in the intestinal mucosa and is phagocytized by macrophages and dendritic cells, in which the bacteria can proliferate.[24] Besides infecting macrophages and dendritic cells, attenuated *S.* Typhimurium, which are facultative anaerobic, have a remarkable tumor-targeting capacity and have been reported to accumulate >1000-fold greater in tumors than other tissues.[25] Attenuated *S.* Typhimurium that carry eukaryotic expression vectors can be used for genetic immunization via the oral route.[26] Attenuated bacteria infect target cells and disrupt after limited proliferation cycles. Antigen-expressing plasmids in the bacterium can be subsequently released into the cytoplasm of the host cell, where they direct expression of the proteins they encode, thus inducing an immune response.[27] Our results showed that *S.* Typhimurium could carry the shRNAs accumulated predominantly in the H22 tumors and effect target gene expression effectively *in vivo*.

HCC is considered to be a hypervascularized tumor and its progression is closely related to angiogenesis.[28] Recent studies have shown that both HIF-1α and VEGF are involved in the malignant transformation of hepatocytes and have an important role at the stage of hepatocarcinogenesis.[29 – 31] In addition, Stat3, an inducer of angiogenesis in terms of upregulating VEGF and HIF-1α,[32] was found to be persistently activated in primary human HCCs[33,34] and appears to have a central role in tumor genesis, this transcription factor is implicated in both oncogenesis and metastasis.[6,34,35] In this study, we found that Stat3 has a key role in promoting HCC proliferation and metastasis *in vivo*. Using the *Salmonella*-delivered shRNAs therapy, our results showed that downregulation of Stat3 powerfully suppresses the growth of H22 tumors and substantially prolongs the survival time of mice by inducing apoptosis and G1 phase arrest. The therapeutic mechanism is due to the inhibition of *Stat3* expression with a coordinated reduction of Stat3-downstream genes in this biopathway. HIF-1α was dramatically reduced by Stat3-shRNA, which resulted in lower VEGF mRNA and protein expression (P<0.01). In addition, the antiapoptotic Bcl-2, cell cycle regulators Cyclin D1 and c-Myc were significantly inhibited in *Salmonella*-Si-Stat3 group compared with the control group. Furthermore, MMP2, which contains a promoter region that directly binds by activated *Stat3*[36] and has been implicated in HCC,[37] is also decreased after Stat3 expression is blocked. Reduction of this multiple proteins results in inhibition of H22 tumor metastasis.

The disturbances of cell proliferation, differentiation and apoptosis are also found on specific signal-transduction pathways within the tumor cells. Besides, the immune system had an important part in it.[38] In our hepatocarcinoma model, treatment with *Salmonella*-delivered Stat3 shRNAs affected multiple immune cells, many of which show enhanced antitumor activity. As innate immunity has an active role in immune surveillance as well as

induced antitumor effects, we investigated whether blocking Stat3 might affect NK cell numbers and their ability to kill target cells. Our finding revealed that the expression and activity of NK cells were greatly improved on day 7 after treated. Additional experiments further assessed the function and expression of T lymphocytes, and our analysis indicated that treatment of *Salmonella*-Si-Stat3 group enhance successively the percentage of $CD8^+$-positive cells, decrease the number of $CD4^+$-positive T cells, and reverse the $CD4^+/CD8^+$ ratio. Tumor cells adapt many always to escape immune surveillance, resulting in immune tolerance to the tumor. $CD4^+CD25^+$ regulatory T cells (Treg) have a crucial role in maintaining self-tolerance in hosts by suppressing a wide variety of immune responses. $CD4^+CD25^+$ Treg populations, originally found to suppress autoimmune responses, are also crucial in controlling antitumor immune responses. We also found a significantly lower number of $CD4^+CD25^+Foxp3^+T_{Treg}$ cells in the treated group as compared with the mock group.

The present study demonstrates that attenuated *S.* Typhimurium can introduce siRNA expression plasmids into H22 tumors, significantly suppressing *Stat3* gene expression and effectively reducing tumor growth and metastasis. In addition, elevated NK cell activity, upregulation of CD8 +T lymphocytes and suppression of Treg cells are partly responsible for the synergistic antitumor effects.

These results further demonstrated the ability of attenuated *S.* Typhimurium to serve as an effective tumor targeting delivery vector for siRNA and provides insight into design of a new therapeutic strategy to improve efficacy of chemotherapy in HCC patients. Finally, a single dose of *Salmonella*-vectored siRNA-Stat3 has revealed in 70% cure rate for orthotopically implanted HCC, which did not recur for an extended 2 years following. These findings offer increased hope that these strategies can be applied to few cancer treatments in humans.

Acknowledgments

We thank Dr EL Hohmann (Massachusetts General Hospital, Harvard Medical School, Boston, MA) for supplying the *S.* Typhimurium strain LH430. This work was funded by the National Natural Science Foundation of China (no. 30801354, no. 30970791), Jilin Provincial Science & Technology Department (no. 20080154), PhD Programs Foundation of Ministry of Education of China (no. 200801831077) and National Cancer Institute Grants CA105005 and CA78282 (DV Kalvakolanu).

References

1. Kamangar F, Dores GM, Anderson WF. Patterns of cancer incidence, mortality, and prevalence across five continents: defining priorities to reduce cancer disparities in different geographic regions of the world. J Clin Oncol. 2006; 24:2137–2150. [PubMed: 16682732]
2. Zender L, Kubicka S. Molecular pathogenesis and targeted therapy of hepatocellular carcinoma. Onkologie. 2008; 31:550–555. [PubMed: 18854656]
3. Thomas M. Molecular targeted therapy for hepatocellular carcinoma. J Gastroenterol. 2009; 44(Suppl 19):136–141. [PubMed: 19148808]
4. Alexia C, Bras M, Fallot G, Vadrot N, Daniel F, Lasfer M, et al. Pleiotropic effects of PI-3′ kinase/Akt signaling in human hepatoma cell proliferation and drug-induced apoptosis. Ann N Y Acad Sci. 2006; 1090:1–17. [PubMed: 17384242]
5. Saxena NK, Sharma D, Ding X, Lin S, Marra F, Merlin D, et al. Concomitant activation of the JAK/STAT, PI3K/AKT, and ERK signaling is involved in leptin-mediated promotion of invasion and migration of hepatocellular carcinoma cells. Cancer Res. 2007; 67:2497–2507. [PubMed: 17363567]
6. Li WC, Ye SL, Sun RX, Liu YK, Tang ZY, Kim Y, et al. Inhibition of growth and metastasis of human hepatocellular carcinoma by antisense oligonucleotide targeting signal transducer and activator of transcription 3. Clin Cancer Res. 2006; 12:7140–7148. [PubMed: 17145839]

7. Gartel AL, Kandel ES. RNA interference in cancer. Biomol Eng. 2006; 23:17–34. [PubMed: 16466964]
8. Gondi CS, Rao JS. Concepts in *in vivo* siRNA delivery for cancer therapy. J Cell Physiol. 2009; 220:285–291. [PubMed: 19391103]
9. Pawelek JM, Low KB, Bermudes D. Tumor-targeted Salmonella as a novel anticancer vector. Cancer Res. 1997; 57:4537–4544. [PubMed: 9377566]
10. Zhang L, Gao L, Zhao L, Guo B, Ji K, Tian Y, et al. Intratumoral delivery and suppression of prostate tumor growth by attenuated Salmonella enterica serovar typhimurium carrying plasmid-based small interfering RNAs. Cancer Res. 2007; 67:5859–5864. [PubMed: 17575154]
11. Ren Z, Gay R, Thomas A, Pae M, Wu D, Logsdon L, et al. Effect of age on susceptibility to Salmonella typhimurium infection in C57BL/6 mice. J Med Microbiol. 2009; 58(Pt 12):1559–1567. [PubMed: 19729455]
12. Hohmann EL, Oletta CA, Killeen KP, Miller SI. phoP/phoQ-deleted Salmonella typhi (Ty800) is a safe and immunogenic single-dose typhoid fever vaccine in volunteers. J Infect Dis. 1996; 173:1408–1414. [PubMed: 8648213]
13. Gao L, Zhang L, Hu J, Li F, Shao Y, Zhao D, et al. Down-regulation of signal transducer and activator of transcription 3 expression using vector-based small interfering RNAs suppresses growth of human prostate tumor *in vivo*. Clin Cancer Res. 2005; 11:6333–6341. [PubMed: 16144938]
14. Zhang L, Gao L, Li Y, Lin G, Shao Y, Ji K, et al. Effects of plasmid-based Stat3-specific short hairpin RNA and GRIM-19 on PC-3M tumor cell growth. Clin Cancer Res. 2008; 14:559–568. [PubMed: 18223232]
15. Leong OK, Muhammad TS, Sulaiman SF. Cytotoxic activities of physalis minima L. chloroform extract on human lung adenocarcinoma NCI-H23 cell lines by induction of apoptosis. Evid Based Complement Alternat Med. 2009
16. Cuevas EP, Escribano O, Monserrat J, Martínez-Botas J, Sánchez MG, Chiloeches A, et al. RNAi-mediated silencing of insulin receptor substrate-4 enhances actinomycin D- and tumor necrosis factor-alpha-induced cell death in hepatocarcinoma cancer cell lines. J Cell Biochem. 2009; 108:1292–1301. [PubMed: 19795387]
17. Dykxhoorn DM. RNA interference as an anticancer therapy: a patent perspective. Expert Opin Ther Pat. 2009; 19:475–491. [PubMed: 19441927]
18. Lee SK, Kumar P. Conditional RNAi: towards a silent gene therapy. Adv Drug Deliv Rev. 2009; 61:650–664. [PubMed: 19394374]
19. Williams BR. Targeting specific cell types with silencing RNA. N Engl J Med. 2005; 353:1410–1411. [PubMed: 16192490]
20. Numnum TM, Makhija S, Lu B, Wang M, Rivera A, Stoff-Khalili M, et al. Improved anti-tumor therapy based upon infectivity-enhanced adenoviral delivery of RNA interference in ovarian carcinoma cell lines. Gynecol Oncol. 2008; 108:34–41. [PubMed: 18061250]
21. Nishikawa H, Sato E, Briones G, Chen LM, Matsuo M, Nagata Y, et al. *In vivo* antigen delivery by a Salmonella typhimurium type III secretion system for therapeutic cancer vaccines. J Clin Invest. 2006; 116:1946–1954. [PubMed: 16794737]
22. Panthel K, Meinel KM, Sevil Domenech VE, Trulzsch K, Russmann H. Salmonella type III-mediated heterologous antigen delivery: a versatile oral vaccination strategy to induce cellular immunity against infectious agents and tumors. Int J Med Microbiol. 2008; 298:99–103. [PubMed: 17719275]
23. Domínguez-Bernal G, Tierrez A, Bartolomé A, Martínez-Pulgarín S, Salguero FJ, Antonio Orden J, et al. Salmonella enterica serovar Choleraesuis derivatives harbouring deletions in rpoS and phoP regulatory genes are attenuated in pigs, and survive and multiply in porcine intestinal macrophages and fibroblasts, respectively. Vet Microbiol. 2008; 130:298–311. [PubMed: 18313237]
24. Sirard JC, Niedergang F, Kraehenbuhl JP. Live attenuated Salmonella: a paradigm of mucosal vaccines. Immunol Rev. 1999; 171:5–26. [PubMed: 10582163]
25. Bermudes D, Low B, Pawelek J. Tumor-targeted Salmonella. Highly selective delivery vectors. Adv Exp Med Biol. 2000; 465:57–63. [PubMed: 10810615]

26. Darji A, Guzmán CA, Gerstel B, Wachholz P, Timmis KN, Wehland J, et al. Oral somatic transgene vaccination using attenuated S. typhimurium. Cell. 1997; 91:765–775. [PubMed: 9413986]
27. Eo SK, Yoon HA, Aleyas AG, Park SO, Han YW, Chae JS, et al. Systemic and mucosal immunity induced by oral somatic transgene vaccination against glycoprotein B of pseudorabies virus using live attenuated Salmonella typhimurium. FEMS Immunol Med Microbiol. 2006; 47:451–461. [PubMed: 16872383]
28. Kuboki S, Shimizu H, Mitsuhashi N, Kusashio K, Kimura F, Yoshidome H, et al. Angiopoietin-2 levels in the hepatic vein as a useful predictor of tumor invasiveness and prognosis in human hepatocellular carcinoma. J Gastroenterol Hepatol. 2008; 23:e157–e164. [PubMed: 17931370]
29. Nakamura K, Zen Y, Sato Y, Kozaka K, Matsui O, Harada K, et al. Vascular endothelial growth factor, its receptor Flk-1, and hypoxia inducible factor-1alpha are involved in malignant transformation in dysplastic nodules of the liver. Hum Pathol. 2007; 38:1532–1546. [PubMed: 17640715]
30. Tanaka H, Yamamoto M, Hashimoto N, Miyakoshi M, Tamakawa S, Yoshie M, et al. Hypoxia-independent overexpression of hypoxia-inducible factor 1alpha as an early change in mouse hepatocarcinogenesis. Cancer Res. 2006; 66:11263–11270. [PubMed: 17145871]
31. Yao DF, Jiang H, Yao M, Li YM, Gu WJ, Shen YC, et al. Quantitative analysis of hepatic hypoxia-inducible factor-1alpha and its abnormal gene expression during the formation of hepatocellular carcinoma. Hepatobiliary Pancreat Dis Int. 2009; 8:407–413. [PubMed: 19666411]
32. Wang M, Tan J, Coffey A, Fehrenbacher J, Weil BR, Meldrum DR. Signal transducer and activator of transcription 3-stimulated hypoxia inducible factor-1alpha mediates estrogen receptor-alpha-induced mesenchymal stem cell vascular endothelial growth factor production. J Thorac Cardiovasc Surg. 2009; 138:163–171. 171 e161. [PubMed: 19577074]
33. Tannapfel A, Anhalt K, Häusermann P, Sommerer F, Benicke M, Uhlmann D, et al. Identification of novel proteins associated with hepatocellular carcinomas using protein microarrays. J Pathol. 2003; 201:238–249. [PubMed: 14517841]
34. Lau CK, Yang ZF, Lam SP, Lam CT, Ngai P, Tam KH, et al. Inhibition of Stat3 activity by YC-1 enhances chemo-sensitivity in hepatocellular carcinoma. Cancer Biol Ther. 2007; 6:1900–1907. [PubMed: 18059167]
35. Yang SF, Wang SN, Wu CF, Yeh YT, Chai CY, Chunag SC, et al. Altered p-STAT3 (tyr705) expression is associated with histological grading and intra-tumour microvessel density in hepatocellular carcinoma. J Clin Pathol. 2007; 60:642–648. [PubMed: 16901975]
36. Xie TX, Wei D, Liu M, Gao AC, Ali-Osman F, Sawaya R, et al. Stat3 activation regulates the expression of matrix metalloproteinase-2 and tumor invasion and metastasis. Oncogene. 2004; 23:3550–3560. [PubMed: 15116091]
37. Sun BS, Dong QZ, Ye QH, Sun HJ, Jia HL, Zhu XQ, et al. Lentiviral-mediated miRNA against osteopontin suppresses tumor growth and metastasis of human hepatocellular carcinoma. Hepatology. 2008; 48:1834–1842. [PubMed: 18972404]
38. Wang T, Niu G, Kortylewski M, Burdelya L, Shain K, Zhang S, et al. Regulation of the innate and adaptive immune responses by Stat-3 signaling in tumor cells. Nat Med. 2004; 10:48–54. [PubMed: 14702634]

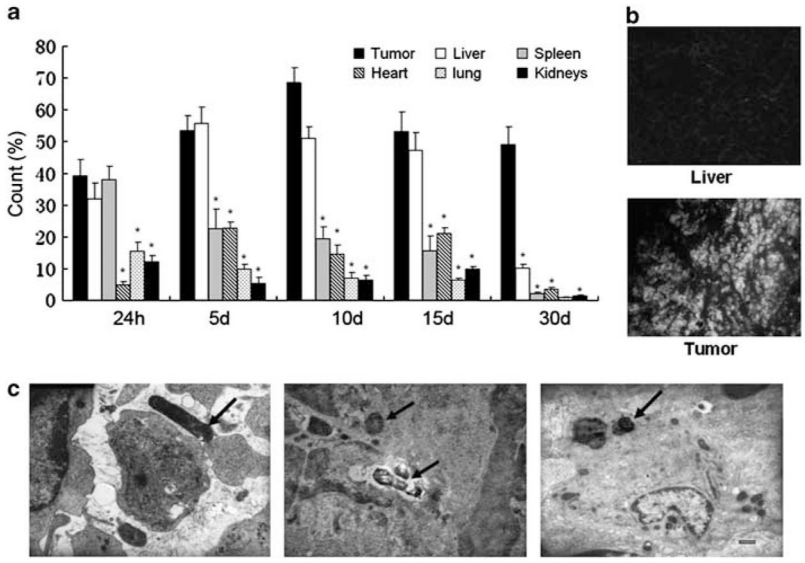

Figure 1.

Recombinant *S*. Typhimurium distribution in C57/BL6 tumor-bearing mice. (**a**) By using GFP expression as a marker, the bacteria distribution in different organ tissues at specified times after inoculation of bacteria (**P*<0.01). (**b**) The GFP expression was observed in tumor and liver tissues by fluorescence microscope. (**c**) Electron microscopic analyses of *S*. Typhimurium infecting H22 tumors. Left panel: bacteria in the intercellular substance of tumor tissues, middle panel: bacteria in the cellular nucleus that was being autolyzed, right panel: bacteria in the tumor-associated macrophage. The arrows indicate the bacteria.

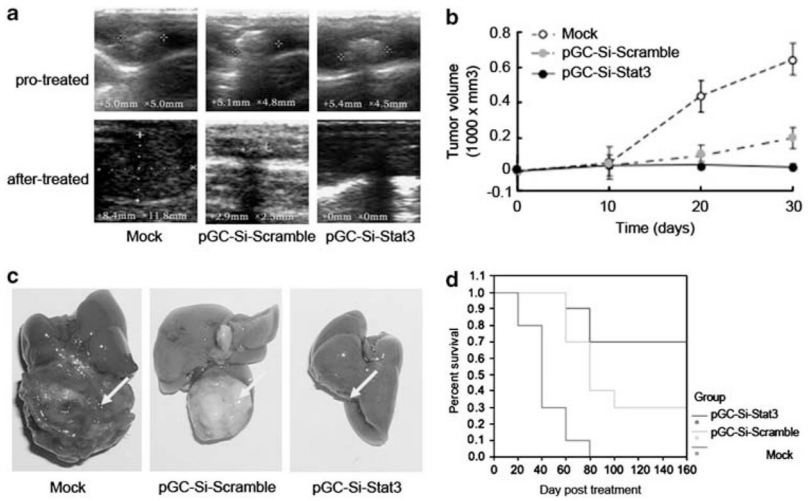

Figure 2.

Inhibition the growth of H22 tumor and prolonging the survival time in C57/BL6 mice by targeting Stat3 carried with *S*. Typhimurium. (**a**) The orthotopic tumors were observed by ultrasonography before and after treatment. (**b**) Growth curves of H22 tumor treated with *Salmonella*-Si-Stat3 measured by ultrasound on days 0, 10, 20 and 30. Points, mean tumor volume (n =10 tumors); bars, s.e. (*P<0.01). (**c**) Relative sizes of s.c. H22 tumors and liver removed from C57/BL6 mice in each treatment group, as indicated after treating for 21 days. Note a total loss of tumor in mice treated with *Salmonella*-Si-Stat3 compared with the control. Arrows indicate tumor locations. (**d**) Survival curves of mice bearing orthotopic H22 tumors following treatment with *Salmonella*-Si-Stat3. The survival time was significantly increased as compared with the control treatment group (*P<0.05).

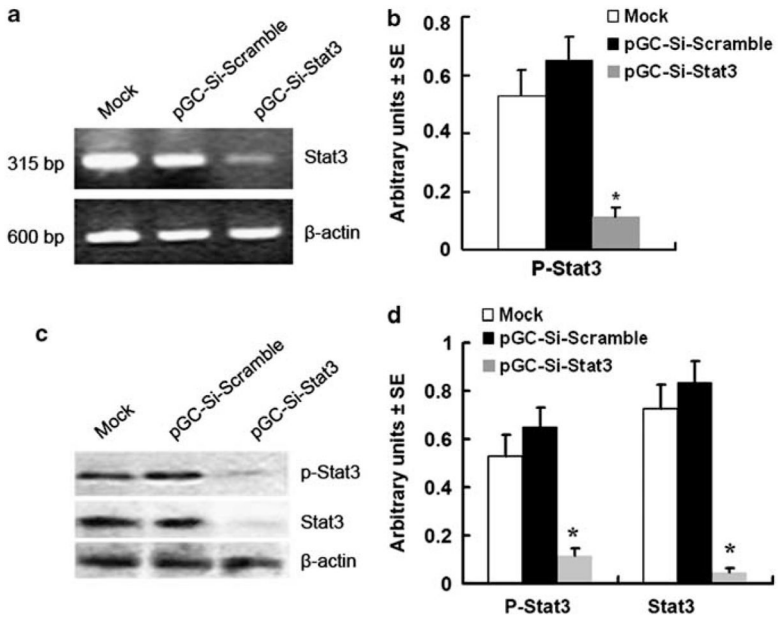

Figure 3.

Inhibition of Stat3 expression by *Salmonella*-Si-Stat3. (**a**) Semi-quantitative RT-PCR analysis. (**b**) Quantification of Stat3 mRNA from three separate experiments, normalized to expression of β-actin. Points, mean; bars, s.e. (**P*<0.01 versus mock and empty vector). (**c**) Western blot analysis. (**d**) Quantification of Stat3 and P-Stat3 protein from three separate experiments, normalized to β-actin (**P*<0.01). Mock-=untreated cells.

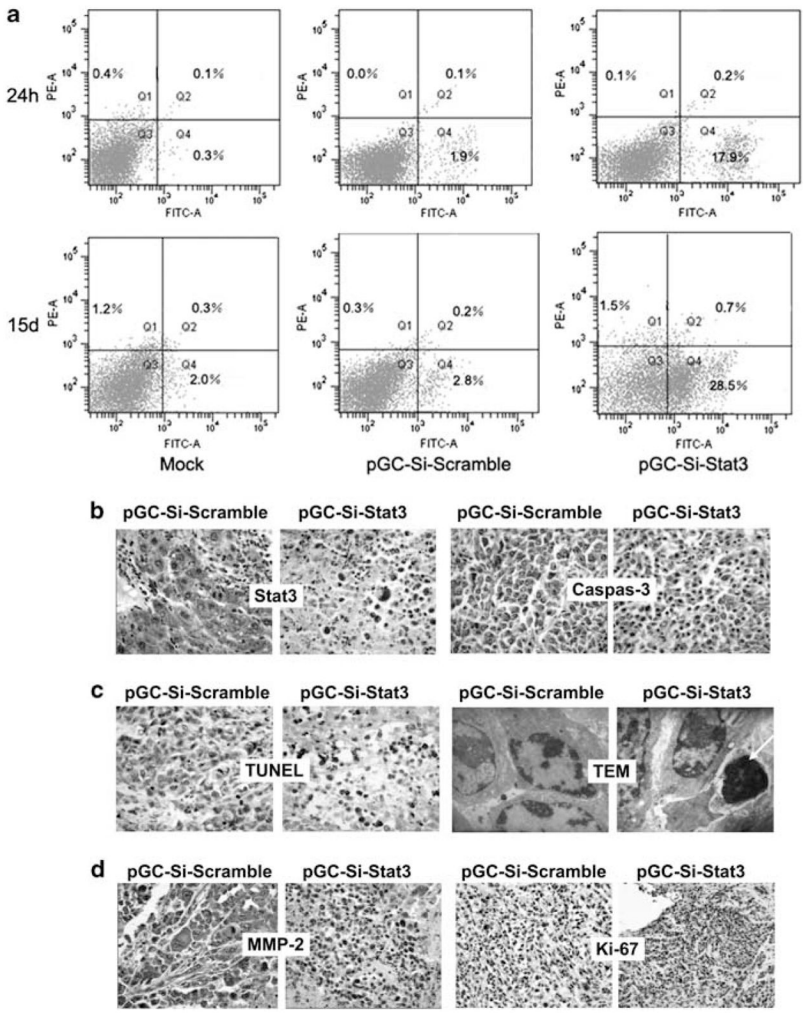

Figure 4.

Salmonella-Si-Stat3 induces H22 tumors apoptosis. (**a**) Flow cytometry analysis of apoptosis cells in H22 tumors following Annexin V-FITC and propidium iodide staining in 24 h and 15 days. (**b**) Immunohistochemical analyses of Stat3 and cleaved caspase-3 expression. Note a strong positive Stat3 and a week negative staining for caspase-3 in pSi-scramble-treated tumor, in sharp contrast to those treated with *Salmonella*-Si-Stat3. Magnification ×400. (**c**) TUNEL staining (magnification ×400) of tumors and ultrastructural feature of apoptotic cells. TUNEL-positive cells (black). Arrowheads point to apoptotic cells, which was exhibit dense nuclei. (**d**) Immunohistochemical analyses of MMP-2 (×400) and Ki-67 (×200) expression. Note a strong positive staining of MMP-2 and Ki-67 in pSi-Scramble-treated tumor, in sharp contrast to those treated with *Salmonella*-Si-Stat3. Q1: dead cells; Q2: early apoptotic cells; Q3: liver cells and Q4: late apoptotic cells.

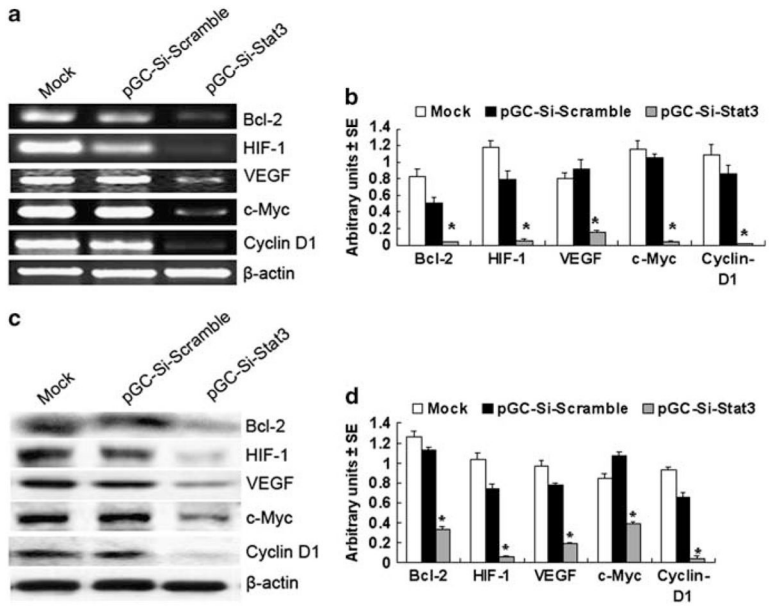

Figure 5.

The expression of Stat3-regulated genes. (**a**) Expression of Bcl-2, HIF-1, VEGF, c-Myc and cyclin D1 mRNA as revealed by semi-quantitative RT-PCR analysis. (**b**) Quantification of Stat3-regulated genes mRNA from three separate experiments, normalized to expression of β-actin. Points, mean; bars, s.e. (**P*<0.01 versus mock and empty vector). (**c**) Western blot analysis of Bcl-2, HIF-1, VEGF, c-Myc and cyclin D1 proteins expression. (**d**) Quantification of Stat3-regulated genes protein from three separate experiments, normalized to β-actin (**P*<0.01). Mock =untreated cells.

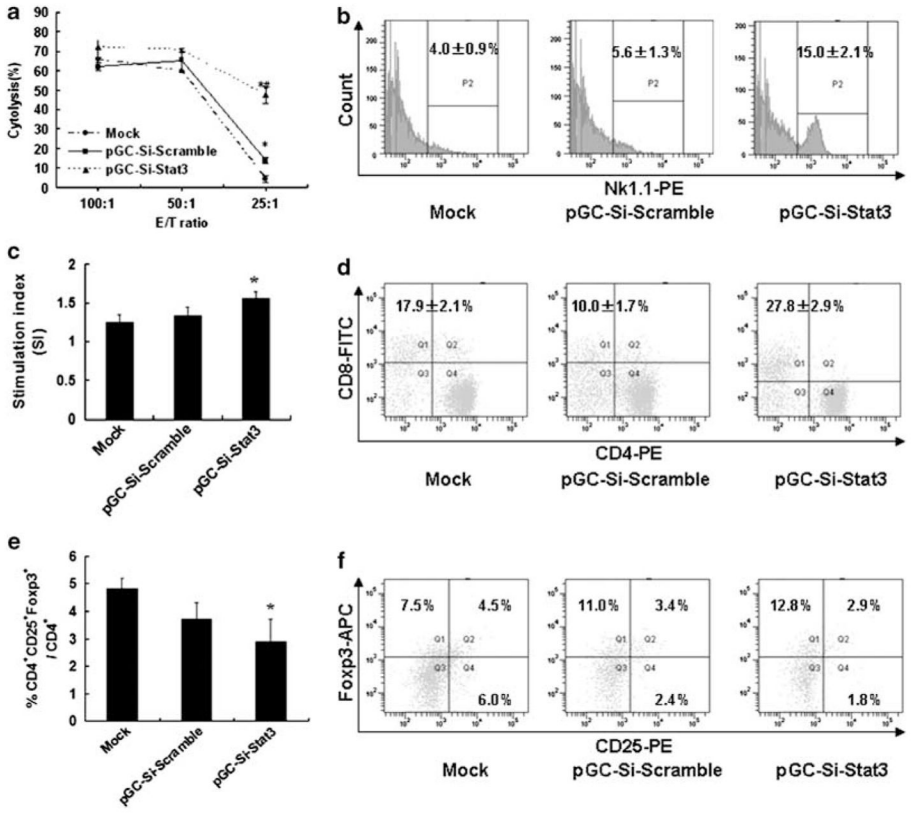

Figure 6.

Salmonella-Si-Stat3 accommodates NK cells and function T lymphocytes function. (**a**) Seven days after inoculation of bacteria, mouse spleens were isolated. Spleenocytes collected and tested for their cytotoxic ability as effector cells. Effector (E) cells were added to target (T) cells (YAC-1) for 18 h at various E/T ratio and NK activity was assessed by the MTT assay. Cytotoxicity against YAC-1 cells showed NK activity. (**b**) Expression of NK cells in spleen was analyzed by flow cytometry in 14 days. P2 indicates gate for NK1.1 positive cells. (**c**) Effect of *Salmonella*-Si-Stat3 on Con A-induced splenic lymphocyte proliferation. MTT colorimetric assay was performed on days 21 of treatment to evaluate T-cell function. Stimulation index (SI) $=OD_{\text{Con A stimulated proliferation}}/OD_{\text{spontaneous proliferation without Con A}}$. (**d**) Responses of T lymphocytes in spleen, as analyzed by flow cytometry in 7 days. (**e**) The percentage of CD4 +CD25 +Foxp3 + T cells was determined by FACS in 14 days. (**f**) The surface expression of CD25 or the intracellular levels of Foxp3 was evaluated in spleenic CD4 + T cells by flow cytometry. Numbers indicate the percentages of cytokine-positive cells in the gates within the total population. $^{*}P<0.05$ versus Mock, $^{\#}P<0.01$ versus pGC-si-Scramble. Abbreviations: APC, allophycocyanin; FITC, fluorescein isothiocyanate; PE, phycoerythrin.

Table 1

Primers used for RT-PCR analysis

Gene	Primers	Expected product size (bp)
Stat3	5′-TTGCCAGTTGTGGTGATC-3′ 5′-AGAACCCAGAAGGAGAAGC-3′	315
Bcl-2	5′-ACTTGACAGAAGATCATGCC-3′ 5′-GGTTATCATACCCTGTTCTC-3′	585
HIF-1	5′-TTATCATGCTTTGGACTCTG-3′ 5′-CCAGCAAAGTTAAAGCATCA-3′	368
VEGF	5′-AGTCCCATGAAGTGATCAAGTTC-3′ 5′-ATCCGCATGATCTGCATGG-3′	220
c-Myc	5′-AGTTGGACAGTGGCAGGG-3′ 5′-ACAGGATGTAGGCGGTGG-3′	237
Cyclin D1	5′-CGCCTTCCGTTTCTTACTTCA-3′ 5′-AACTTCTCGGCAGTCAGGGGA-3′	256
β-Actin	5′-ATATCGCTGCGCTGGTCGTC-3′ 5′-AGGATGGCGTGAGGGAGAGC-3′	517

Table 2

The comparison of the body weight of the C57BL/6 mice, tumor weight, tumor volume of liver cancer

Group (n =10)	Mean weight (g)		Mean tumor Volume (mm^3)	Metastases (%)		
	Mouse	Tumor		Peritoneal seeding	Bloody ascites	Lung
Mock	26.78±4.52	2.42±1.37	2274.09±1735.17	90	100	100
Salmonella alone	25.14±2.98	0.91±0.78[a]	589.23±426.75[a]	40	30	30
pGC-Si-Scramble	25.02±2.47	0.75±0.44[a]	551.98±367.01[a]	30	20	20
pGC-Si-Stat3	24.44±2.13	0.43±0.49[a,b]	301.99±390.16[a,b]	0	0	0

[a] $P<0.01$ versus mock.

[b] $P<0.01$ versus pGC-Si-Scramble.